IEEE EMC Society Letters on Electromagnetic Practice and Applications

Behavioral Modeling of an Off-the-Shelf Damped Sinusoidal Transient Generator

Xiaokang Liu, *Member, IEEE*, Flavia Grassi, *Senior Member, IEEE*, François Trotti, and Werner Hirschi

***Abstract*—In this paper, experimental characterization and behavioral modeling of an off-the-shelf damped sinusoidal wave generator operating at different frequencies are addressed. Two modeling strategies are developed which lead to an active and a passive circuit representation of the generator, whose involved parameters are optimized by making use of time-domain measurement results obtained with the generator connected to different load impedances. It is shown that either the active or the passive model can assure accurate prediction of the generated waveforms, depending on the specific frequency. The proposed models can be effortlessly implemented in common circuit simulators, and used for systematic design of injection devices for transient conducted susceptibility testing as well as for simulation of the corresponding test setups. As an illustrative example, the proposed models are exploited to predict the actual waveform induced at the input pins of the device under test in a simplified pulse current injection test setup.**

***Index Terms*—Behavioral modeling, damped oscillatory wave generator, injection device, sinusoidal transients.**

I. INTRODUCTION

In order to test the vulnerability of electrical/electronic units to intense transient electromagnetic disturbances, such as those due to high-altitude (HEMP) or lightning (LEMP) electromagnetic pulses, several aerospace and military standards foresee both radiated and conducted procedures to induce at the input pins of the device under test (DUT) a stress waveform with assigned characteristics [1]-[3]. The pertinent setups [4]-[6] usually resort to inductive or capacitive couplers [5] to inject specified transient disturbances into the cables connected with the DUT. For instance, the exploited inductive couplers are very similar to the probes used for bulk current injection, and are usually manufactured by winding the inner conductor around a toroidal ferrite/nano-crystalline magnetic core. However, assuring that the actual waveform induced at the DUT input exhibits the characteristics specified by the standards requires the use of specific instrumentation (e.g., injection probes with suitable characteristics as well as *ad-hoc* generators) as well as proper test procedures. Towards this goal, accurate modeling of the exploited test setup is a prerequisite for further investigations.

This work presents the results obtained in the framework of a joint

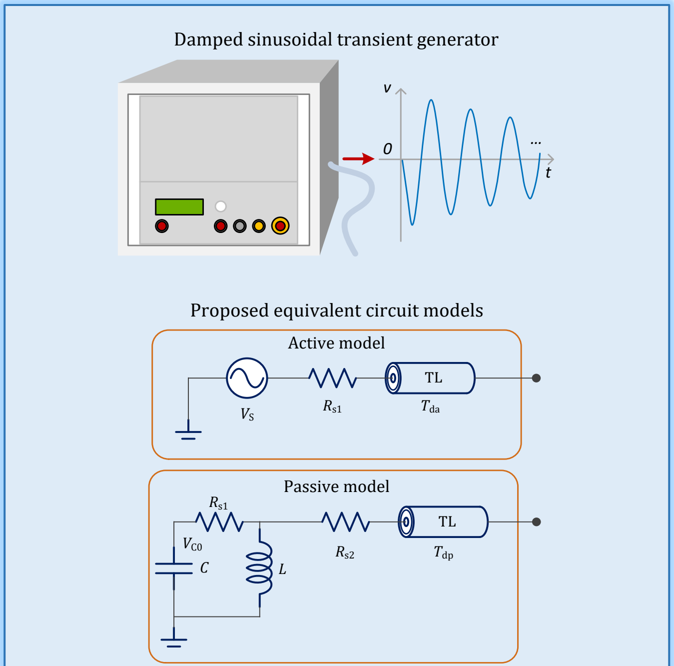

Off-the-shelf damped sinusoidal (DS) generator (top panel) and the proposed circuit models. (Visual Summary)

research activity between Montena Technology (Switzerland) and the EMC Group at Politecnico di Milano (Italy). The final objective is to develop novel modelling strategies that guide the design of injection devices with enhanced characteristics in terms of maximum amplitude of the (peak) current that can be injected into the DUT. Particularly, this work focuses on the injection of damped sinusoidal (DS) transients according to the procedures and waveforms defined in the standard MIL-STD-461 [2], section "Conducted Susceptibility (CS) Test

Take-Home Messages:

- Damped sinusoidal (DS) generators are key-instruments in HEMP and LEMP setups, and their modelling allows controlling the actual stress waveform at the DUT input during the test.
- DS generators contain sources at different frequencies, and each source needs to be modelled.
- Despite the lack of information on their internal structure, behavioral models allowing for accurate predictions can be obtained starting from measurement data.
- The effectiveness of the two modelling strategies here proposed depends on the frequency of the DS source.
- The proposed models can be used to predict the stress waveforms induced by pulse current injection, as well as to improve the design of the involved injection probes.

X. Liu and F. Grassi are with the Department of Electronics, Information and Bioengineering, Politecnico di Milano, 20133 Milan, Italy (e-mail: xiaokang.liu@polimi.it; flavia.grassi@polimi.it).

F. Trotti and W. Hirschi are with Montena Technology sa, 1728 Rossens, Switzerland (e-mail: francois.trotti@montena.com; werner.hirschi@montena.com).

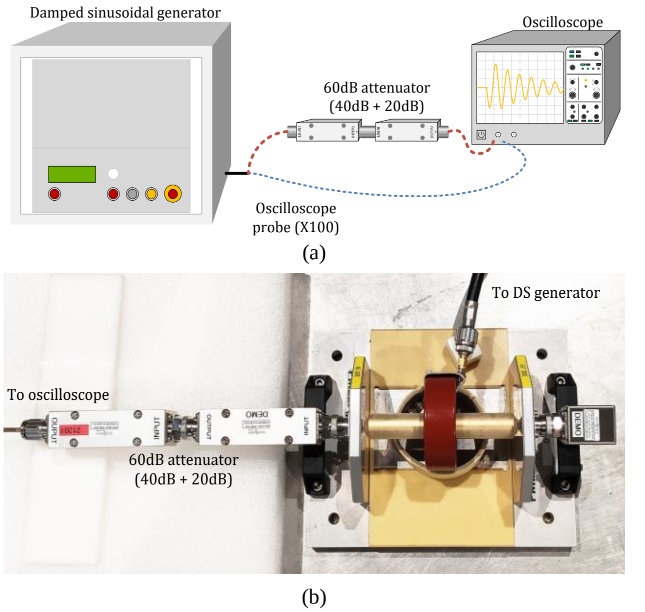

Fig. 1. Test schemes for DS generator when terminated with (a) 50-Ω (red path) or high-impedance load (blue path), and (b) an *ad-hoc* injection coupler with a nanocrystalline magnetic core and a calibration jig.

CS116: Damped Sinusoidal Transients, Cables & Power Leads", with the objective to develop behavioral models of the involved DS generators. These generators allow immunity verification of cable-connected system in a wide frequency interval and embed distinct internal circuits to generate specific waveforms at discrete (up to 17) test frequencies. As a result, developing accurate circuit model representative for their behavior for different working frequency and under different loading conditions is a challenge.

Despite the inherent difficulty imposed by the presence of different internal circuits (one for each specific waveform, i.e., frequency), this work proposes two behavioral modeling strategies, which involve frequency-dependent parameters evaluated starting from the measurement data obtained operating the generator at different frequencies and with different loads. The proposed models are then validated in a simplified setup for pulsed current injection.

II. Basic Characteristics of the Waveform

According to MIL-STD-461 CS116 standard, damped sinusoidal transients are defined within the frequency interval from 10 kHz to 100 MHz [2] to simulate electrical current and voltage waveforms occurring in platforms from excitation of natural resonances. The standard requires to verify the ability of the DUT to withstand DS transients coupled onto DUT-associated cables and power leads. A normalized current waveform is specified by the Standard as [2]

$$I(t) = I_p \cdot e^{-\frac{\pi f t}{Q}} \sin(2\pi f t) \tag{1}$$

where I_p is the peak current in the first cycle, f is the sinusoidal frequency in Hertz, and Q is the damping factor (15±5).

In this work, a prototype of commercial DS generator, i.e., model POG-CS116-17 [7] conforming to CS116 requirements, is tested and modeled. Various frequencies are available by switching the internal sources (through a control interface), which are connected to the same generator output. This allows generating waveforms with different frequencies and pulse shapes without the need for re-cabling or exchanging modules. Among them, in this work the generator sources at three specific frequencies, i.e., 100 kHz, 1 MHz, and 10 MHz, are modeled. In all cases, the voltage level is set to a defined value. For each frequency, the generator is characterized by time-domain measurement of the outlet voltage by realizing two different loading conditions [see Fig. 1(a)]. In the first case, the generator output is directly connected to the oscilloscope, thus leading to a 50 Ω load (i.e., input impedance of the scope). In the second case, a ×100 high-voltage probe is used for connection with the oscilloscope input, thus leading to a loading condition approaching an open circuit (i.e., 66.7 MΩ). In this latter case, the input impedance of the oscilloscope is set to 1 MΩ to match the probe specifications.

From the measurement results in Fig. 2, it is possible to observe that the output voltage is a sinusoidal waveform with exponentially decaying amplitude as long as a 50-Ω load is connected. Conversely, for high-impedance loads, it may significantly deviate from the theoretical waveform depending on the frequency. At 100 kHz, the voltage is nearly identical to the 50 Ω load case; at 1 MHz, a reduced damping w.r.t. to the theoretical waveform is observed; at 10 MHz, the actual waveform is significantly distorted owing to reflections and propagation along the cable. These characteristics imply different implementations of the internal sources and, as a consequence, the need for different equivalent circuits.

III. Equivalent Circuits and Parameter Optimization

To reproduce the behavior of the DS generator, two modeling strategies are here proposed, leading to the two circuit models shown in the Visual Summary.

- The first model, so-called "active model" in the top panel, involves an active source V_S with parametric time-domain expression, in addition to the internal source resistance R_{S1};
- The second model, so-called "passive model" in the bottom panel, involves passive components only, and requires to specify the initial voltage across the capacitor C to generate the desired output waveform.

In both circuits, ideal transmission lines with characteristic

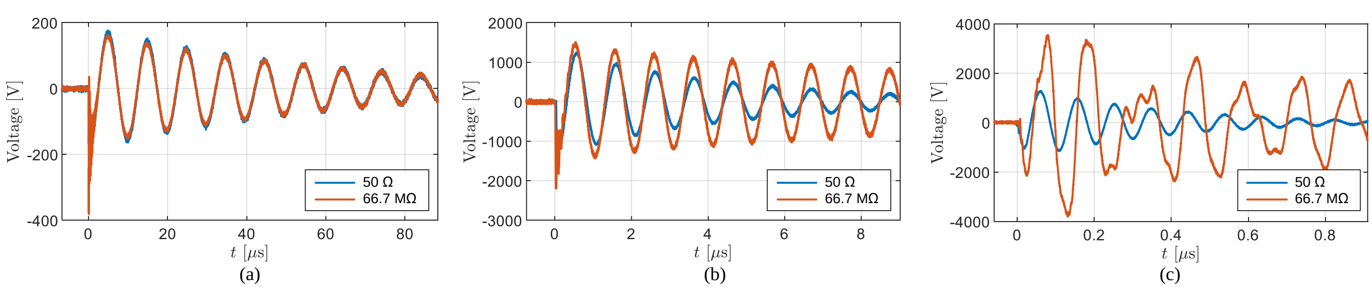

Fig. 2. Measurements of the output voltage for two different loading conditions and (a) 100 kHz, (b) 1 MHz, and (c) 10 MHz DS sources. Results are properly scaled according to the applied attenuations.

IEEE EMC SOCIETY | Letters on Electromagnetic Practice and Applications

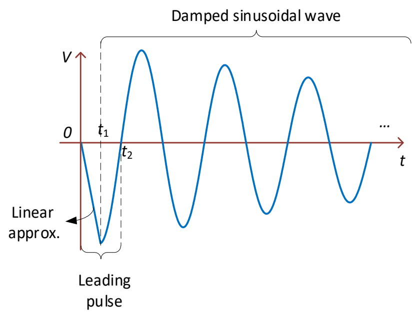

Fig. 3. Approximation of the DS source waveform (active model).

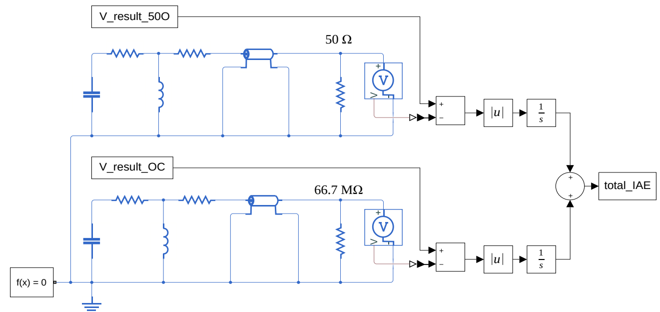

Fig. 4. Simulink diagram for the optimization of the parameters of the passive model of the DS generator.

impedance 50 Ω are included to account for the effects introduced by the external RG214 cable (approximately 5 meters), which are non-negligible especially at 10 MHz and in the presence of high-impedance terminations, Fig. 2(c).

For the active model, a two-step optimization procedure is proposed, foreseeing to evaluate the parameters describing the voltage source waveform as the first step, and the value of R_{S1} subsequently. To this end, V_s is assigned a parametric analytical expression, starting from the experimental observation that the initial part of the generated waveform (see Fig. 3) does not exactly obey (1), but exhibits a leading pulse, which can be better represented by a linear approximation. Accordingly, the following expression is cast:

$$V_s(t)=\begin{cases} kt,\ 0\le t\le t_1 \\ V_m e^{-\frac{\pi(f_N+\Delta f)(t-t_2)}{Q+\Delta Q}}\sin\left[2\pi\left(f_N+\Delta f\right)\left(t-t_2\right)\right],\ t\ge t_1 \end{cases} \quad (2)$$

which follows (1) for $t>t_1$ only. In this expression, k denotes the slope of the leading pulse and can be determined according to the values of $V_s(t_1)$ and t_1, as $k=V_s(t_1)/t_1$; V_m is the voltage amplitude; f_N is the nominal frequency (i.e., 100 kHz, 1 MHz, and 10 MHz); Δf is the frequency variation (set equal to ±10% of f_N for the optimization); Q_N=15 is the nominal damping factor; ΔQ denotes the damping factor variation ($-5\le\Delta Q\le+5$); t_1 and t_2 are used to describe the duration of the leading pulse. The initial optimization is aimed at determining Δf and ΔQ. To this end, the voltage measured across the 50 Ω load (pre-processed using a median filter to suppress random noise) is used. As the first step, the waveform is fitted, by ignoring the leading pulse through the expression:

$$V_s'(t)=V_m'\cdot e^{-\frac{\pi(f_N+\Delta f)t}{Q_N+\Delta Q}}\sin\left[2\pi\left(f_N+\Delta f\right)t\right] \quad (3)$$

where superscripts denote quantities of the DS part of (2).

After optimization by a *pattern search* strategy (implemented in MATLAB), optimal values for V_m', Δf, and ΔQ are obtained. Δf and ΔQ are considered to be constant in the subsequent optimization, which is carried out by a Simulink-based simulation model with the objective to evaluate the other parameters, including: t_1, t_2, V_m (starting from the initial guess of V_m' obtained in the previous step), and R_{S1} and T_{da}, i.e., the internal impedance and the time delay introduced by the RG214 cable, respectively (see Visual Summary).

Specifically, at each iteration the values determined by the optimization algorithm are applied to the Simulink-based simulation model, which makes use of the *Simscape Electrical* module [8] to simulate the circuit. For each combination of parameters, the voltage waveforms across the 50-Ω and high-impedance loads are evaluated and compared versus the measured waveforms. The total integral absolute error (IAE) between the measured and simulated waveforms is computed as output of the Simulink model and considered as the quantity to be minimized. The optimization algorithm converged to the global minimum of IAE for the set of parameters in Tab. I.

Table 1: Active Model: Optimal Parameters

Parameter	100 kHz source	1 MHz source	10 MHz source
V_m / V	170.904	2174.25	1435.972
Δf / Hz	1192.984	-23807	390852
ΔQ	3.084	-1.071	-4.041
T_{da} / ns	37.612	25.067	33.733
R_{S1} / Ω	2.456	37.273	0.971
t_1 / ns	70	2.5	2.0
t_2 / μs	2.51	0.259	3.508

Table 2: Passive Model: Optimal Parameters

Parameter	100 kHz source	1 MHz source	10 MHz source
V_{C0} / V	183.688	1505.813	1523.438
C / nF	683.458	60.872	18.212
L / μH	3.615	0.435	0.0127
R_{S1} / Ω	0.122	0.0619	0.062
R_{S2} / Ω	2.283	7.877	1.314
T_d / ns	37.161	13.329	33.107

Moving from the active to the passive model, once a proper circuit topology has been established (see bottom panel in the Visual Summary), optimal values for the involved circuit elements are obtained by directly resorting to a single-step optimization procedure. The Simulink model exploited for parameter optimization is shown in Fig. 4, and the obtained component values are collected in Table 2.

As a preliminary validation, the waveforms measured in the setup shown in Fig. 1(a) are compared versus those predicted by the two models in Fig. 5. The comparison shows that, depending on the source frequency, one model can be more accurate than the other, depending on the different physical implementations of the internal sources. For instance, the 100 kHz DS is accurately described by the active model, whereas the passive model introduces an over-damping in the 50 Ω load case. For the 1 MHz source, the passive model provides accurate predictions for both loads, whereas the active model leads to discrepancies w.r.t. measurement for high-impedance loads. For the 10 MHz source, the two models provide results in satisfactory agreement with measurement, with the active model slightly outperforming the passive one for high-impedance loads.

IEEE EMC SOCIETY Letters on Electromagnetic Practice and Applications

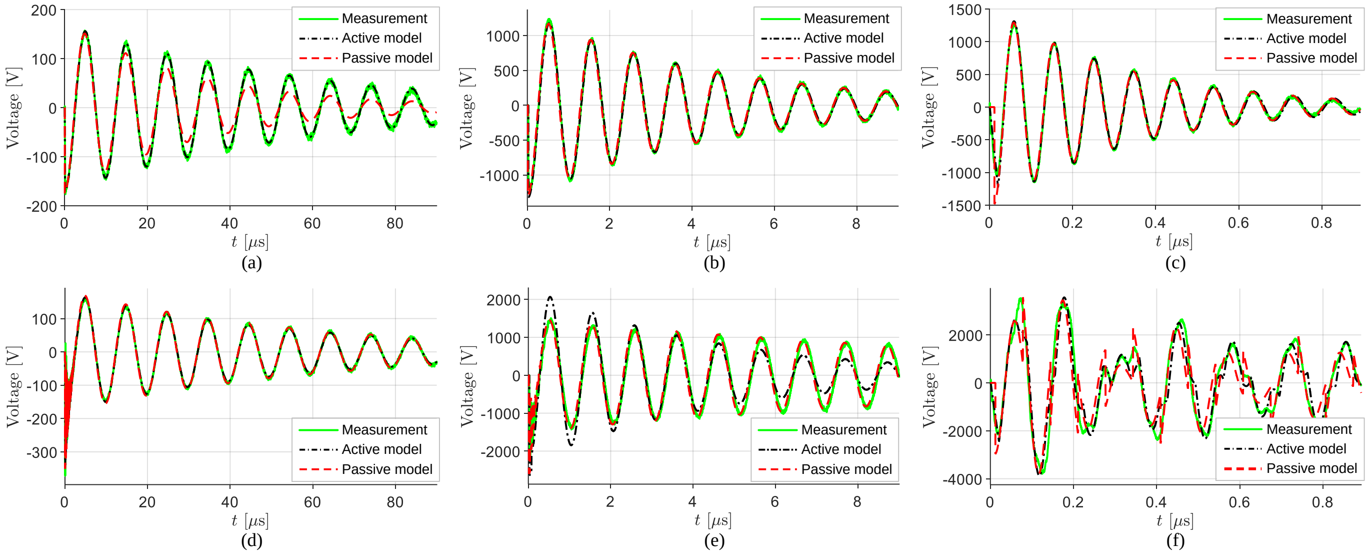

Fig. 5. Measurement and simulation of the output voltage for 100 kHz, 1 MHz, and 10 MHz DS sources. (a)-(c): 50 Ω load; (d)-(f): 66.7 MΩ load.

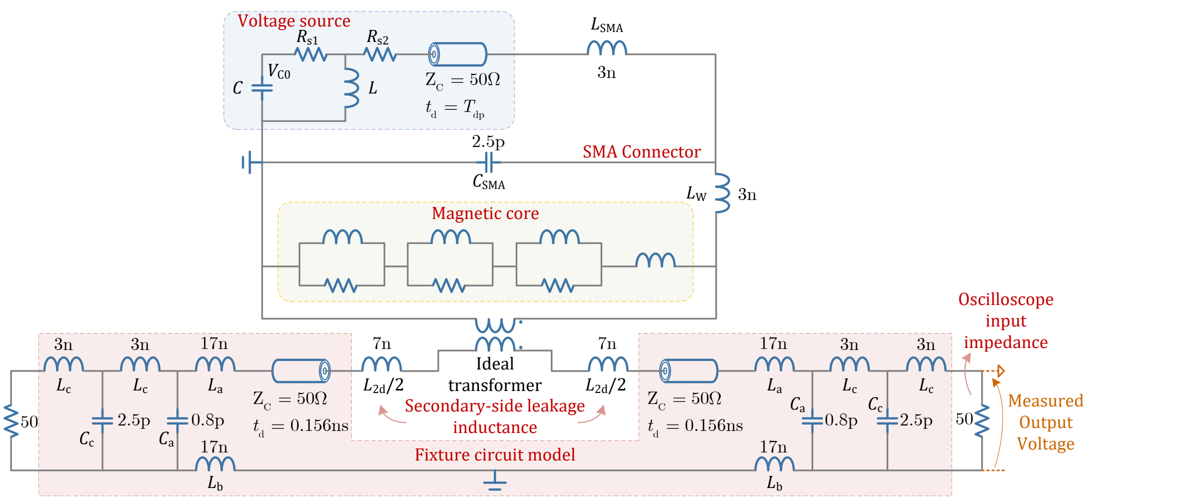

Fig. 6. Circuit model of the whole injection setup used for time-domain simulation. The DS generator is here represented by the passive model as an example.

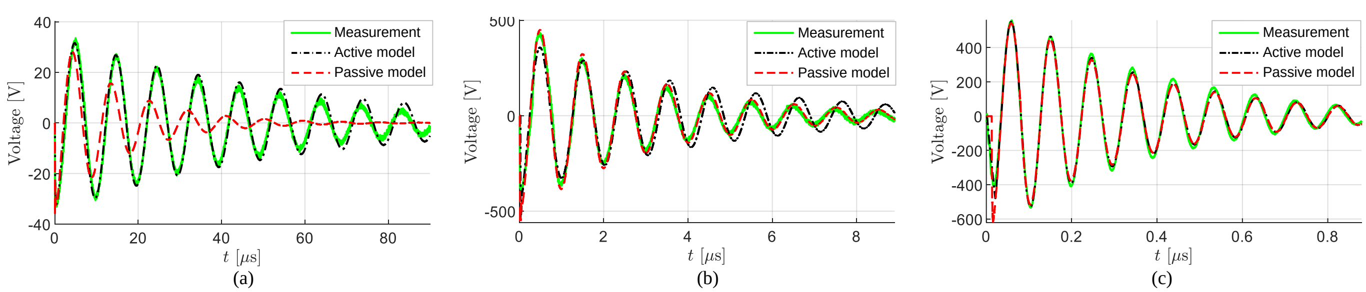

Fig. 7. Measurement and prediction of the voltage induced in the injection setup in Fig. 1(b): (a) 100 kHz DS source, (b) 1 MHz DS source, and (c) 10M DS source.

IV. Application Example

As an illustrative example of application, the models of the DS generator previously presented are here used to predict the voltage induced across a 50 Ω load in a simplified setup mimicking a pulsed current injection test bench. To this end, a hand-made inductive coupler is manufactured by winding a thin copper tape, equipped with an SMA connector, around a nanocrystalline magnetic core. Such a probe was experimentally characterized, and modeled in [9], where equivalent ladder networks were derived to represent its frequency response in the linear region. The probe is mounted onto the center conductor of a commercial calibration jig, [10], whose ports are connected to a 50 Ω termination on one side [right-side in Fig. 1(b)], and to the oscilloscope channel on the other side [left-side in Fig. 1(b)]. The circuit model of the overall setup used for time-domain simulation is shown in Fig. 6, where the passive model of the DS generator is shown as an example. The parameters of the ladder network representing the magnetic core, here omitted for simplicity, can be found in [9].

For measurement, a higher voltage was set for the DS sources at 1 and 10 MHz, whereas for the 100 kHz source the selected level was

IEEE EMC SOCIETY | Letters on Electromagnetic Practice and Applications

lower to avoid saturation of the magnetic core. To predict the voltage induced at the monitored termination of the jig, a Simulink-based model was exploited which combines the proposed models of the DS generator with the probe and jig models in [9] and [10], respectively. Predictions and measurements of the induced voltage are compared in Fig. 7. These results prove the accuracy of the proposed modeling strategies, and confirm the conclusions drawn in the previous section, that is, one model may be more accurate than the other depending on the specific frequency of the DS source.

V. CONCLUSION

In this manuscript, two modelling strategies have been proposed to predict the actual waveforms generated by off-the-shelf DS generators conforming to MIL-STD-461 CS116 requirement. The first model, active model, makes use of a parametric analytic expression of the open-ended DS equivalent voltage source. The second model, passive model, only involves passive components, and requires to set the initial voltage across an inside capacitor. Both models do not require any knowledge on the internal circuit structure of the generator, yet the involved model parameters are obtained by processing the measurement data at the generator output by MATLAB/Simulink-based optimization routines.

Although not shown here for brevity, the proposed models can be easily implemented also in other simulation environments, such as SPICE, and used not only to predict and control the stress waveforms induced during the test at the DUT input, but also to improve the design of the involved injection devices, as proven by the validation example described in Section IV.

REFERENCES

[1] *High-Altitude Electromagnetic Pulse (HEMP) Protection for Ground Based C4i Facilities Performing Critical Time-Urgent Missions*, MILSTD-188-125-1, 2005.

[2] *Requirements for the Control of Electromagnetic Interference Characteristics of Subsystems and Equipment*, MIL-STD 461F, Dec. 2007.

[3] *Electromagnetic Compatibility (EMC)–Part 4: Testing and Measurement Techniques – HEMP Immunity Test Methods for Equipment and Systems*, IEC-61000-4-25, 2001.

[4] Z. Cui, F. Grassi, S. A. Pignari and B. Wei, "Pulsed current injection setup and procedure to reproduce intense transient electromagnetic disturbances," *IEEE Trans. Electromagn. Compat.*, vol. 60, no. 6, pp. 2065-2068, Dec. 2018.

[5] Y. Zhou, Y. -Z. Xie, D. -Z. Zhang and Y. Jing, "Modeling and performance evaluation of inductive couplers for pulsed current injection," *IEEE Trans. Electromagn. Compat.*, vol. 63, no. 3, pp. 710-719, June 2021.

[6] Y. -H. Chen, Y. -Z. Xie, D. -Z. Zhang *et al.*, "10-kV transmission line experimental platform for HEMP immunity test of electrical equipment in operation," *IEEE Trans. Power Deliv.*, vol. 36, no. 2, pp. 1034-1040, April 2021.

[7] Montena sa., "CS116 Damped sinusoid generator datasheet: POGCS116." Accessed: July 21, 2021. [Online]. Available: https://www.montena.com/fileadmin/technology_tests/documents/data_sheets/Data_sheet_POGCS116.pdf

[8] The MathWorks Inc., "Simscape Electrical." Accessed: July 21, 2021. [Online]. Available: https://www.mathworks.com/products/simscape-electrical.html

[9] X. Liu, F. Grassi, G. Spadacini *et al*., "Behavioral modeling of complex magnetic permeability with high-order Debye model and equivalent circuits," *IEEE Trans. Electromagn. Compat.*, vol. 63, no. 3, pp. 730-738, June 2021.

[10] X. Liu, L. Crosta, F. Grassi *et al.*, "SPICE modeling of probes for pulse current injection," in *Proc. IEEE ESA Workshop Aerosp. EMC*, May 2019, pp. 1–6.